A New Manipulability Measure for the Control of CRAM: A Cable-driven Remote Access Manipulator

Wilhelm Johan Marais[1], **Ali Haydar Göktoğan**[2]
The School of Aerospace, Mechanical and Mechatronic Engineering[1,2]
Australian Centre for Field Robotics[2]
The University of Sydney, Australia
wmar5627@uni.sydney.edu.au[1], a.goktogan@acfr.usyd.edu.au[2]

Abstract

Kinematically redundant serial manipulators are often used for operation in constrained environments, due to the high degree of articulation and extended operational capabilities provided by the additional Degrees of Freedom (DoF). This paper presents the control method for a novel 12-DoF Cable-driven Remote Access Manipulator (CRAM) for confined spaces inspection. The system is designed such that each DoF is coupled to a single motor, and can bend $\pm 90°$ for a large range of motion. The control of CRAM is through an iterative inverse kinematics solution based on the manipulator Jacobian. Self-motion is computed for joint angle limit avoidance. A new normalised manipulability measure, called the "Weighted Harmonic Isotropy Measure" (WHIM), is also presented. It is based on the Harmonic Mean Manipulability Index (HMMI) and the Measure of Isotropy, and is shown to outperform other commonly used normalised indices in terms of stability near singularities. Simulations with user defined control inputs demonstrate that the inverse kinematics scheme effectively achieves the desired pose, while avoiding large joint angles.

1 Introduction

Serial manipulators with a high number of kinematically redundant Degrees of Freedom (DoF) offer several advantages over those with limited DoF [Charles A. Klein, 1983]. These advantages include the ability for simultaneous obstacle avoidance and task motion, singularity avoidance, as well as the realisation of highly flexible motion. Hence, they can be used in constrained environments and confined spaces with a limited volume, poor accessibility, and/or poor ventilation [Horigome *et al.*, 2014; Buckingham and Graham, 2010].

Kinematic redundancy creates difficulties in solving for the inverse kinematics of a manipulator due to the lack of deterministic solutions [Chan and Lawrence, 1988]. Thus many kinematic solutions require the use an iterative method based on the manipulator Jacobian [Charles A. Klein, 1983; Chan and Lawrence, 1988; Mayorga *et al.*, 1992]. Kinematic solutions based on the Jacobian suffer from instability at singularities, and therefore selective damping based on a measure of manipulability are often used [Chiaverini *et al.*, 1994].

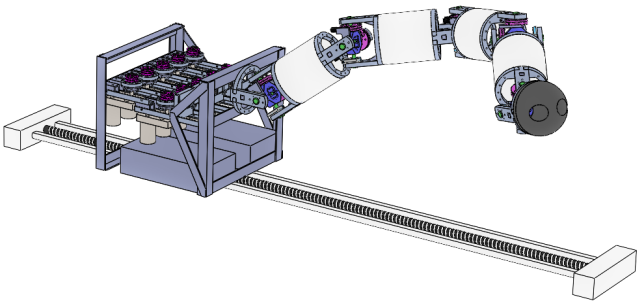

Figure 1: A 3D model of the proposed 12 DoF CRAM system, showing the translating base, 2 DoF joints and replaceable end effector

The large number of DoFs of redundant serial manipulators requires the use of many actuators. This leads to excessive distributed weight, which can be overcome through the use of a tendon driven (also known as cable driven) mechanism. This effectively removes the need to lift the weight of actuators, which are placed in the base of the system. A manipulator which transmits force through a tendon mechanism often suffers from the introduction of non-linearities and coupling of DoF.

Many existing tendon driven systems for inspection take the form of remote access manipulators, referring to the ability of a manipulator to access confined spaces while mounted external to the environment.

OC Robotics X125 is a high tension tendon driven manipulator [Buckingham and Graham, 2010] which uses a universal joint mechanism. The system has 2-DoF per joint, which increases the degree of articulation and

range of motion. More than two actuators are required per 2-DoF joint which creates complex actuator kinematic coupling. Coupled tendon designs [Horigome *et al.*, 2014; S. Hirose, 1991] require only one actuator per DoF. A coupled tendon mechanism refers to the direct coupling of two opposing tendons joint to the same actuator. These systems have a reduced degree of articulation compared to a universal joint system since each joint only has 1-DoF. A 24-DoF system with a coupled tendon mechanism [Dong *et al.*, 2017] was introduced for on wing aircraft inspection. Despite the large number of DoF, each joint has a limited bending range, reducing the workspace of the system and the total bending angle.

The kinematic structure of a 12-DoF Cable-driven Remote Access Manipulator (CRAM) is presented in Figure 1, combining a coupled tendon design and two degree of universal joints [Marais and Göktoğan, 2017]. Each DoF is independently controlled by a single actuator using a Bowden tube design, and realises bending angles of $\pm 90°$. The contributions of this paper include a control scheme for the kinematically redundant CRAM. A variable damping factor is used, and a new manipulability measure for singularity detection is introduced. The measure is extended to include a weighting factor based on the desired task manipulability requirements, with the final measure called the Weighted Harmonic Isotropy Measure (WHIM). This measure is applicable to a wide range of manipulators, yet is initially analysed here within the CRAM framework.

Section 2 recalls a damped Jacobian pseudoinverse kinematics control scheme, with selective damping based on the distance to singularities. Additionally a new manipulability measure is introduced to better represent the distance to a singular configuration, and a null space control scheme for joint limit avoidance is presented. Simulation results are provided in Section 3. Finally, the conclusions are summarised in Section 4.

2 Kinematics

2.1 Forward Kinematics

The forward kinematics of CRAM was solved using standard Denavit-Hartenberg (DH) parameters. CRAM consists of 1 prismatic joint q_1 for linear translation of the base, and 11 revolute joints q_2 – q_{12}. The coordinate frames used are shown in Figure 2, where q_1 is along the z axis of frame $\{1\}$ and q_2 – q_{12} are along the z axes of frames $\{2\}$ – $\{12\}$. The DH parameters are tabulated in Table 1. Using standard pose transformations, the forward kinematics function f can be found as

$$\mathbf{x} = f(\mathbf{q}) \tag{1}$$

where $\mathbf{x} = (x, y, z, \theta_x, \theta_y, \theta_z) \in \Re^m$ is the pose vector of the end effector in the task space, and $\mathbf{q} = (q_1 ..... q_{12}) \in \Re^n$ is the joint configuration vector in the configuration space.

Table 1: Table of standard DH parameters

Link	$\mathbf{d_j}$ (mm)	$\boldsymbol{\theta_j}$ (rads)	$\mathbf{a_j}$ (mm)	$\boldsymbol{\alpha_j}$ (rads)	Joint Limit (mm) or (rads)
1	d_1	$\pi/2$	105	$-\pi/2$	0-1300
2	0	$-\pi/2 + \theta_2$	0	$\pi/2$	$-\pi/2$ - $\pi/2$
3	0	θ_3	250	$-\pi/2$	$-\pi/2$ - $\pi/2$
4	0	θ_4	0	$\pi/2$	$-\pi/2$ - $\pi/2$
5	0	θ_5	250	$-\pi/2$	$-\pi/2$ - $\pi/2$
6	0	θ_6	0	$\pi/2$	$-\pi/2$ - $\pi/2$
7	0	θ_7	250	$-\pi/2$	$-\pi/2$ - $\pi/2$
8	0	θ_8	0	$\pi/2$	$-\pi/2$ - $\pi/2$
9	0	θ_9	250	$-\pi/2$	$-\pi/2$ - $\pi/2$
10	0	θ_{10}	0	$\pi/2$	$-\pi/2$ - $\pi/2$
11	0	$\pi/2 + \theta_{11}$	0	$\pi/2$	$-\pi/2$ - $\pi/2$
12	69	$\pi + \theta_{12}$	0	0	$-\pi/2$ - $\pi/2$

2.2 Inverse Kinematics

The inverse kinematics problem involves finding the function f^{-1} which maps from the task space to the configuration space.

$$\mathbf{q} = f^{-1}(\mathbf{x}) \tag{2}$$

Kinematically redundant manipulators are defined as have a larger configuration space than task space, or $n > m$. Therefore (1) will consist of n equations with m unknowns, and will in general be an under-determined system with an infinite set of solutions in $\Re^{n-m}$.

The lack of an analytical method means numerical methods exist using the Jacobian [Chan and Lawrence, 1988; Mayorga *et al.*, 1992; Chiaverini *et al.*, 1991].

Taking the derivative with respect to time of (1) yields

$$\dot{\mathbf{x}} = J\dot{\mathbf{q}} \tag{3}$$

where J is the Jacobian matrix which maps from joint velocities to pose velocities. The inverse of J only exist for non-singular square matrices. For the kinematically redundant case where J is an $m \times n$ matrix, the Moore-Penrose pseudoinverse [Charles A. Klein, 1983] can be taken to give

$$\dot{\mathbf{q}} = J^{+}\dot{\mathbf{x}} \tag{4}$$

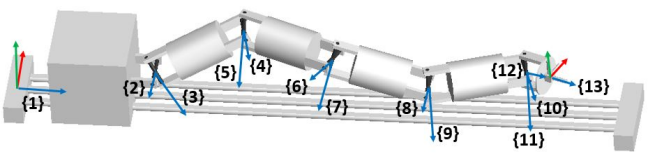

Figure 2: A simplified model of the 12-DoF CRAM system showing the setup of coordinate frames with x, y, and z, where frame $\{1\}$ is the base frame and $\{13\}$ is the end effector frame

where J^+ is the Jacobian pseudoinverse. This effectively finds the minimum Euclidean norm solution to (3), or the shortest path in $\mathbf{q}$ space.

This can be discretised to give

$$\Delta\mathbf{q} = J^+\Delta\mathbf{x} = J^+(\mathbf{x}_d - \mathbf{x}_c) \tag{5}$$

which is valid approximation for small iteration steps. The end effector pose error is $(\mathbf{x}_d - \mathbf{x}_c)$, the difference between the desired and current end effector pose.

The Jacobian for CRAM takes the form

$$\begin{aligned} J &= \begin{pmatrix} \partial x_1/\partial q_1 & \cdots & \partial x_1/\partial q_{12} \\ \vdots & \ddots & \vdots \\ \partial x_6/\partial q_1 & \cdots & \partial x_6/\partial q_{12} \end{pmatrix} \\ &= \begin{pmatrix} z_1 & z_2 \times p_2 & \cdots & z_{12} \times p_{12} \\ 0 & z_2 & \cdots & z_{12} \end{pmatrix} \end{aligned} \tag{6}$$

where $z_1, \cdots, z_{12}$ are the joint axes for frames $\{1 \cdots 12\}$ with respect to frame $\{1\}$, and $p_1, \cdots, p_{12}$ are the vectors from frames $\{1 \cdots 12\}$ to the end effector frame $\{13\}$ with respect to frame $\{1\}$. Each value of z and p can be found using forward kinematics and DH parameters for any configuration.

The Moore-Penrose pseudoinverse [Charles A. Klein, 1983] takes the form

$$J^+ = J^T(JJ^T)^{-1} \tag{7}$$

where J^T is the transpose of the Jacobian J.

2.3 Singularity Detection and Stability

A singularity occurs when the dimension of the vector space to which the Jacobian maps is less than the dimension of the task space m. This can be alternatively stated as $Rank(J) < m$. At singular configurations, the determinant of JJ^T is zero and the calculation of the pseduinverse given in (7) is no longer valid.

Approaching singularities, joint velocities are required to approach infinity to produce changes in end effector position in degenerate directions [Mayorga *et al.*, 1992]. Stability at singularities refers to a control scheme which limits high joint velocities for desired changes in end effector pose in degenerate directions.

The use of a damped pseudoinverse [Mayorga *et al.*, 1992; Chiaverini *et al.*, 1994; 1991] places a lower bound on the determinant of JJ^T by adding elements to the diagonal to yield the damped equation for the pseudoinverse

$$J^+ = J^T(JJ^T + \lambda I_m)^{-1} \tag{8}$$

where λ is a positive constant and I_m is the $m \times m$ identity matrix. This creates errors in the control scheme leading to non-straight paths in the task space and longer convergence times. This is undesirable in confined spaces where well defined motion is required.

A variable damping factor [Chan and Lawrence, 1988; Chiaverini *et al.*, 1994] can be used to provide fast convergence and stability at singularities. The suggested method [Mayorga *et al.*, 1992] is for a variable damping factor based on an estimate of the distance to a singularity.

$$\lambda = \begin{cases} \lambda_{max}(1 - \frac{M}{M_0}) & M \leq M_0 \\ 0 & M > M_0 \end{cases} \tag{9}$$

where M is a local measure of manipulability, M_0 is a constant tuning parameter to prevent damping at high manipulability, and λ_{max} is the maximum damping factor.

The definition of manipulability is given in [Patel and Sobh, 2015] as the ability of a manipulator to move and apply forces in any desired direction in the task space.

The commonly used measure of the distance to a singularity is Yoshikawa's manipulability measure [Yoshikawa, 1985]. This measure is based on the manipulator Jacobian. Combining elements for both prismatic and revolute joints within the Jacobian makes it non-homogeneous [Patel and Sobh, 2015] due to a mismatch between units. Therefore to solve this issue, the Jacobian elements for prismatic and revolute joints are considered separately, as well as separate consideration for translational and rotational velocities [Patel and Sobh, 2015]. Jacobian elements for revolute joints and translational velocities are considered exclusively for the remainder of this paper, yet the same measures can be applied to prismatic joints and rotational velocities.

Yoshikawa's measure, μ, is given by

$$\mu = \sqrt{det(JJ^T)} \tag{10}$$

where μ is proportional to the volume of the velocity ellipsoid. The velocity ellipsoid represents the end effector velocity in the task space for unit Euclidean norm $\mathbf{q}$ [Yoshikawa, 1985]. The measure can also be written as $\mu = \sigma_1 ... \sigma_m = \sqrt{\omega_1 ... \omega_m}$ where σ are the singular values of J, or the radii of the velocity ellipsoid, and ω are the eigenvalues of JJ^T. Large singular values represent a high end effector velocity for unit Euclidean norm joint velocity in the corresponding direction. Likewise, small singular values correspond to directions of high force transmission and accuracy [Patel and Sobh, 2015].

Yoshikawa's measure has been criticized for being a poor measure of the manipulability [Patel and Sobh, 2015]. This limitation occurs since the volume of the velocity ellipsoid does not necessarily decrease near singularities as one of the radii becomes small, if other radii become larger. The measure μ also suffers from order dependancy, since it has dimensions of $velocity^m$ and therefore gives different units for manipulators of different task space dimensions. Finally, μ is also unbounded

and scale dependent making it difficult to use as a comparative measure for different manipulators.

The Local Conditioning Index (LCI) [Kucuk and Bingul, 2006; Cardou *et al.*, 2010] is defined as

$$LCI = \frac{\sigma_{min}}{\sigma_{max}} = \sqrt{\frac{\omega_{min}}{\omega_{max}}}, \qquad \in [0,1]. \tag{11}$$

the ratio of the minimum and maximum singular values σ or equivalently, the square roots of the ratio of the minimum and maximum eigenvalues ω. It provides a measure of the spatial uniformity or isotropy of the velocity ellipsoid. A limitation of the method is that it only considers motion in 2 directions, unlike the index μ which considers all of the radii of the velocity ellipse. Another limitation of the LCI is that it can not be written analytically as a function of $\mathbf{q}$.

To remove the order and scale dependency, Yoshikawa's measure μ was extended [Kim and Khosla, 1991]. First to remove the order dependency, it was suggested to use $M = \sqrt[m]{det(JJ^T)}$, the geometric mean of the eigenvalues ω, which has units of $velocity^2$. Next to remove scale dependency, this was divided by the arithmetic mean of the eigenvalues, also of units $velocity^2$, to give

$$\Delta = \frac{\sqrt[m]{det(JJ^T)}}{\frac{tr(JJ^T)}{m}}, \qquad \in [0,1]. \tag{12}$$

where tr is the trace of a matrix. The trace of JJ^T is simply the sum of the eigenvalues ω. Δ is known as the Measure of Isotropy and is a normalised and unitless measure of manipulability. Isotropy refers to the degree of directional uniformity of the velocity ellipsoid. This measure is not as sensitive as the LCI for singularity detection, as shown in Figure 3, where Δ indicates relatively high isotropy at near singular values. The geometric mean provides an average of a set of numbers of different numeric ranges, and therefore is not an appropriate metric in this case, where all eigenvalues are over the same numeric range.

The Harmonic Mean Manipulability Index (HMMI) [Hashimoto, 1985] was introduced to provide a measure which is dominated by small eigenvalues. The measure was introduced to solve the issue of Yoshikawa's measure μ, which may not reflect when a singular value approaches zero if the other singular values increase. The HMMI is given by,

$$HMMI = \sqrt{\frac{1}{tr[(JJ^T)^{-1}]}} \tag{13}$$

This measure is not bounded and also suffers from scale dependency.

2.4 A New Manipulability Measure

A new manipulability measure is presented based on Δ and the HMMI.

$$\Delta_H = \frac{H}{A}, \qquad \in [0,1] \tag{14}$$

where H is the harmonic mean of the eigenvalues,

$$H = \frac{m}{\frac{1}{\omega_1} + ... \frac{1}{\omega_m}} = \frac{m}{tr[(JJ^T)^{-1}]} \tag{15}$$

and A is the arithmetic mean,

$$A = \frac{\omega_1 + ... + \omega_m}{m} = \frac{tr(JJ^T)}{m} \tag{16}$$

The rationale behind the use of the harmonic mean is that it provides a method of averaging rates of change, which is what the eigenvalues of JJ^T represent. The measure can be written as

$$\Delta_H = \frac{\frac{m}{tr[(JJ^T)^{-1}]}}{\frac{tr(JJ^T)}{m}} \tag{17}$$

This measure is bounded between 0 and 1, is neither scale nor order dependant, and can be written analytically as a function of $\mathbf{q}$.

Figure 3 shows a comparison of the normalised indices, LCI, Δ and Δ_H, for $\omega_1 \in [0,1]$ and $\omega_2 = \omega_3 = 1$. It can be seen that the gradients of the LCI and Δ approach infinity towards the singular configuration at $\omega_1 = 0$, while Δ_H becomes linear (approaches $m^2/2$). Therefore Δ_H gives a clearer indication of the distance to a singularity due to its linear nature near singularities.

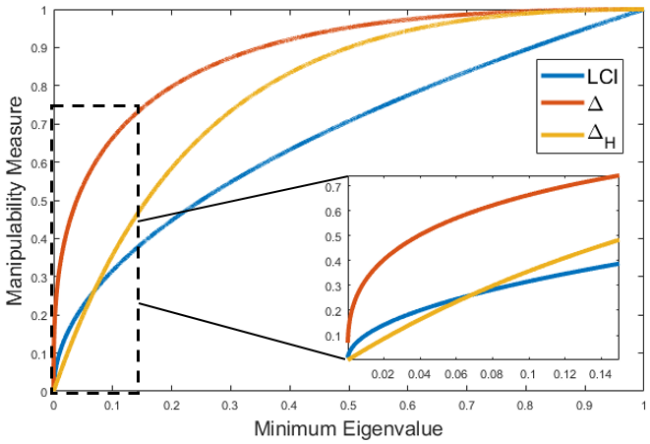

Figure 3: Graph of LCI, Δ and Δ_H manipulability measures as a function of the minimum eigenvalue ω_1, with $\omega_2 = \omega_3 = 1$

Figure 4 shows the use of the LCI, Δ and Δ_H manipulability measures for evaluation of a variable damping coefficient λ according to (9). The plot shows

$det(JJ^T + \lambda I)^{-1}$, which provides a measure of the magnitude of the velocity commands given by the inverse kinematics scheme, with $\lambda_{max} = 0.02$ and $H_0 = 0.1$. It can be seen that with $\lambda = 0$, the magnitude of the velocity commands approaches infinity at singularities, as expected. Using Δ as a measure, the lack of a reliable metric for the distance to a singularity leads to poor damping of large velocity commands. Comparing the use of the LCI to Δ_H, the use of the LCI leads to larger maximum velocity commands, and irregular damping near singularities.

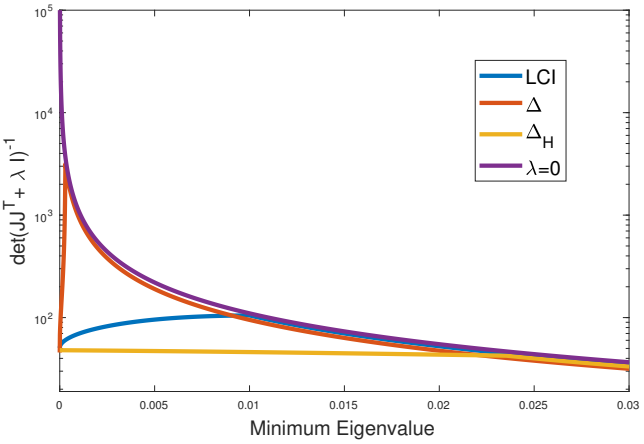

Figure 4: Graph of $det(JJ^T + \lambda I)^{-1}$ using LCI, Δ and Δ_H manipulability measures for damping, as a function of the minimum eigenvalue ω_1, with $\omega_2 = \omega_3 = 1$

Addition of a Weighting Factor

The Δ_H measure can be extended to include a weighting factor W,

$$\Delta_W = \frac{\frac{tr(W)}{tr[W^2(JJ^T)^{-1}]}}{\frac{tr(JJ^T)}{tr(W)}} \qquad \in [0,1] \tag{18}$$

where W is a square symmetric matrix of size $m \times m$ formed by taking AA^T for some matrix A.

W defines the task ellipsoid [Cloutier *et al.*, 1994; Dubey and Luh, 1988], or the ellipsoid which represents the desired velocity and force transmission characteristics. A proof of the boundedness of Δ_W can be found in the appendix. This measure is called the Weighted Harmonic Isotropy Measure (WHIM). An example of the use of a task ellipsoid can be seen in Figure 5 were the desired task is to insert a round peg into a hole. High precision is required in the x and y directions, while a large degree of movement is required in the z direction. Therefore in the example given in Figure 5,

$$W = \begin{pmatrix} 1 & 0 & 0 \\ 0 & 1 & 0 \\ 0 & 0 & 10 \end{pmatrix} \tag{19}$$

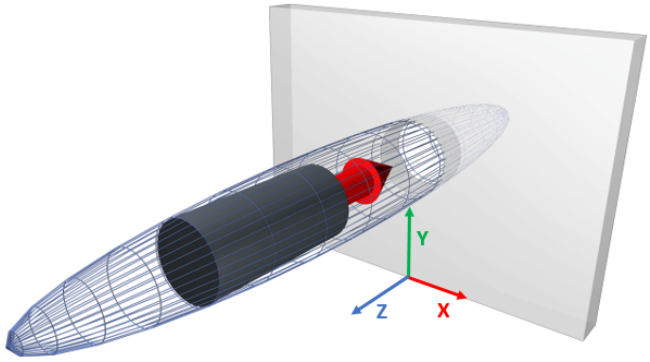

Figure 5: An example of the use of a task ellipsoid for an operation in which a peg has to be inserted into a hole

It should be noted that only the relative size of the elements in W matter as the measure is invariant to the scale of the task ellipsoid.

The final variable damped pseudoinverse implementation for the CRAM system uses to unweighted measure Δ_H, to give

$$\lambda = \begin{cases} \lambda_{max}(1 - \frac{H}{H_0}) & \Delta_H \leq H_0 \\ 0 & \Delta_H > H_0 \end{cases} \tag{20}$$

H_0 and λ_{max} were tuned experimentally to provide stability at singular configurations and fast convergence of the inverse kinematics scheme.

2.5 Self Motion for Joint Limit Avoidance

For kinematically redundant manipulators, a set of $n-m$ null space vectors exist which are orthogonal to the output space. The null space of J is the space of homogenous solutions to (3). This allows self motion to be computed, which has no effect on the pose of the end effector, yet violates the minimum Euclidean norm constraint given by the pseudoinverse [Charles A. Klein, 1983]. The control scheme now becomes

$$\Delta\mathbf{q} = J^+\Delta\mathbf{x} + \alpha(J^+J - I_n)\,H(\mathbf{q},t) \tag{21}$$

where I_n is the $n \times n$ identity matrix, $(JJ^+ - I_n)$ is the orthogonal projection onto the null space, α is a positive gain constant, and $H(\mathbf{q},t)$ is some optimisation $n \times 1$ vector function. The Jacobian pseudoinverse J^+ is damped as per (8) with the damping factor computed in (20).

The form of $H(\mathbf{q},t)$ can be used for null space singularity avoidance, yet the form of a vector which can avoid singularities over the entire domain is an unsolved problem [Mayorga *et al.*, 1992]. The use of null space motion for joint limit avoidance [Charles A. Klein, 1983] is given as

$$H(\mathbf{q},t) = max(\mathbf{q} - \mathbf{q}_c) \tag{22}$$

where $\mathbf{q}_c$ is the centre of each joint position. The CRAM implementation included a threshold for each joint to limit self motion at small joint angles, which would lead to a straightening of all joints and hence a singularity.

$$H(\mathbf{q},t) = \begin{cases} sgn(\mathbf{q})\ max|\mathbf{q}|, & max|\mathbf{q}| > \frac{\pi}{4} \\ 0 & max|\mathbf{q}| \leq \frac{\pi}{4} \end{cases} \tag{23}$$

where the centre of motion for each joint is 0. Here the function *max* returns a velocity vector containing only the maximum joint angle, and *sgn* preserves the required direction of motion for angle minimisation. For prismatic joint q_1 responsible for base translation, the measure was scaled as

$$q_1 \rightarrow \left(\frac{q_1}{q_{c1}} - 1\right)\frac{\pi}{2} \tag{24}$$

where q_{c1} is the centre of q_1, to create consistent joint scaling.

The gain constant α was tuned to provide effective limiting motion, without creating instability.

3 Simulation Results

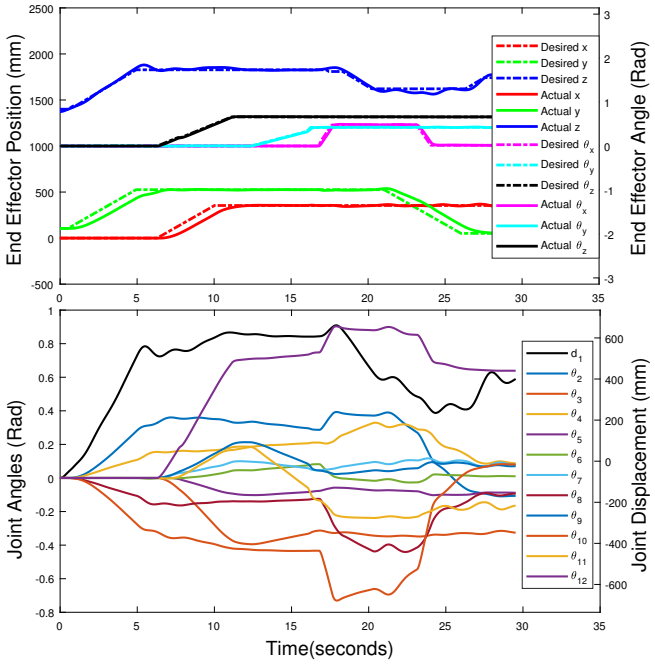

Figure 6: Graph of desired pose vs actual pose (top), with joint angles (bottom) showing effectiveness of self motion for joint angle reduction

The 12-DoF CRAM system was simulated on MATLAB/Simulink to confirm the validity of the inverse kinematics scheme. A full spatial desired pose $\mathbf{x}_d$ was provided via a gamepad input during the simulation.

A graph of the desired pose $\mathbf{x}_d$ and actual pose $\mathbf{x}_c$ is shown in the top plot of Figure 6. The pseudoinverse control scheme effectively converges to the user defined desired pose inputs. The use of a variable damping factor leads to fast pose convergence times, while limiting high joint velocities over the entire manipulator workspace.

The bottom plot of Figure 6 shows the linear displacement d_1 of the prismatic joint q_1, and joint angles θ_2 – θ_{12}, of joints q_2 – q_{12}. The null space motion is shown to effectively keep the joint angles within the mechanical limits of $\pm\frac{\pi}{2}$, and the prismatic joint q_1 between 0mm and 1300mm. Due to the dead-zone for self motion, the joint angles aren't forced to approach 0, limiting the occurrence of singularities.

A comparison of the LCI, Δ and Δ_H measures during the CRAM simulation are shown in Figure 7. Each measure correctly confirms the initial singular configuration. It can be seen that Δ is a poor indicator of the near presence of a singularity as is evident between 20 and 30 seconds. To provide damping in this region, a threshold of $M_0 = 0.4$ would have to be implemented. This would lead to unnecessarily damping at configurations which may not be near singular. The linear nature of Δ_H at small eigenvalues leads to a better indication of a near singularity between 20 and 30 seconds than the LCI and Δ. In particular, Δ_H only gives a smaller manipulability value near singular configurations, and larger values away from singularities. Thus implementing damping thresholds for the two measures will lead to more selective damping when using Δ_H compared to the LCI. This confirms the results of Figure 3, and the validity of the use of Δ_H as a normalised index for variable Jacobian damping.

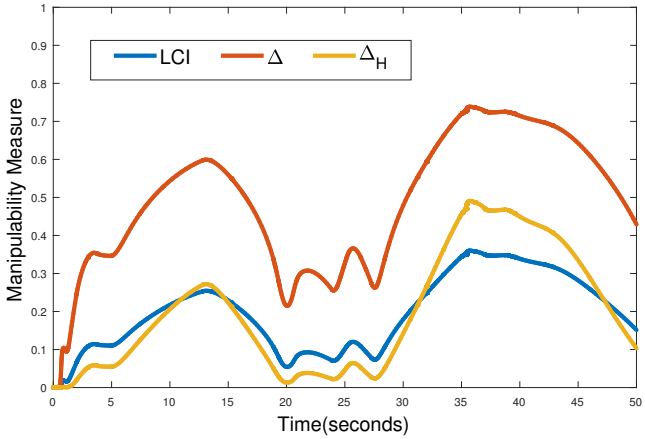

Figure 7: Graph of LCI, Δ and Δ_H manipulability measures during CRAM simulation

4 Conclusion

An inverse kinematics solution for a Cable-driven Remote Access Manipulator (CRAM) for confined spaces inspection was presented. The inverse kinematics was solved using an iterative solution based on the manipulator Jacobian and shown to converge to user defined pose inputs in simulation. Through null space motion, the joints are shown to avoid mechanical limits.

To overcome instability at singularities, a damped pseudoinverse control scheme is used, with variable damping based on a measure of manipulability. A new manipulability measure is proposed which is bounded, scale and order independent, and can be written in an analytical form. The measure is shown to give desirable results for determining the distance to a singularity compared to both the Local Conditioning Index (LCI) and the Measure of Isotropy. Using the measure for pseudoinverse damping is shown to give more regular damping characteristics. The measure is extended to include a weighting factor based on the task ellipsoid and the final measure is called the Weighted Harmonic Isotropy Measure (WHIM).

The WHIM presents many further opportunities. The derivation of an analytical expression of the WHIM for CRAM or any redundant robotic manipulator, would allow for joint configuration optimisation based on the desired task. Since the measure is normalised, it also allows for the comparison of different manipulator structures, and hence structure optimisation. The WHIM can also be extended for use as a global manipulability measure to allow for configuration optimisation across the entire manipulator workspace.

5 Appendix

Proof. The aim is to show that $\Delta_W \in [0,1]$ for all W and J. The measure is clearly greater than 0 since all elements are positive.

To prove for an upper bound of 1, (18) can be simplified and hence the problem reduces to proving that

$$tr[W^2(JJ^T)^{-1}]\, tr(JJ^T) \geq tr(W)^2 \tag{25}$$

Now taking the singular value decomposition of J gives

$$\begin{aligned} tr[W^2(JJ^T)^{-1}] &= tr[W^2U\Sigma\Sigma^TU^T] \\ tr[U^TWW^TU\Sigma\Sigma^T] &= \\ tr[(U^TWU)(U^TWU)^T\Sigma\Sigma^T] & \end{aligned} \tag{26}$$

where U is a unitary matrix, Σ is diagonal singular matrix, and the cyclic invariance properties of the trace of a matrix have been used.

Therefore the left hand side of (20) can be expressed in terms of the singular values σ of J as

$$\sum_{i=1}^{m} \frac{d_i}{\sigma_i^2} \sum_{i=1}^{m} \sigma_i^2 \tag{27}$$

where d_i are the diagonal elements of $(U^TWU)(U^TWU)^T$.

$$\begin{aligned} \sum_{i=1}^{m} \frac{d_i}{\sigma_i^2} \sum_{i=1}^{m} \sigma_i^2 &\geq \Big(\sum_{i=1}^{m} \frac{\sqrt{d_i}\sigma_i}{\sigma_i}\Big)^2 \\ &= \Big(\sum_{i=1}^{m} \sqrt{d_i}\Big)^2 \end{aligned} \tag{28}$$

by the Cauchy-Schwarz inequality.

$$\Big(\sum_{i=1}^{m} \sqrt{d_i}\Big)^2 \geq \Big(\sum_{w=1}^{m} d_w\Big)^2 \tag{29}$$

where d_w are the diagonals of U^TWU.

$$\Big(\sum_{w=1}^{m} d_w\Big)^2 = \Big(\sum_{w=1}^{m} \lambda_w\Big)^2 = tr(W)^2 \tag{30}$$

where λ_w are the eigenvalues of W. □

References

[Buckingham and Graham, 2010] R. O. Buckingham and A. C. Graham. Dexterous manipulators for nuclear inspection and maintenance - Case study. In *2010 1st International Conference on Applied Robotics for the Power Industry*, pages 1–6, Oct 2010.

[Cardou *et al.*, 2010] P. Cardou, S. Bouchard, and C. Gosselin. Kinematic-sensitivity indices for dimensionally nonhomogeneous jacobian matrices. *IEEE Transactions on Robotics*, 26(1):166–173, Feb 2010.

[Chan and Lawrence, 1988] S. K. Chan and P. D. Lawrence. General inverse kinematics with the error damped pseudoinverse. In *Proceedings. 1988 IEEE International Conference on Robotics and Automation*, pages 834–839 vol.2, Apr 1988.

[Charles A. Klein, 1983] Ching-Hsiang Huang Charles A. Klein. Review of pseudoinverse control for use with kinematically redundant manipulators. In *IEEE Transaction on Systems, Man, and Cybernetics*, pages 245 – 250, March 1983.

[Chiaverini *et al.*, 1991] S. Chiaverini, O. Egeland, and R. K. Kanestrom. Achieving user-defined accuracy with damped least-squares inverse kinematics. In *Advanced Robotics, 1991. 'Robots in Unstructured Environments', 91 ICAR., Fifth International Conference on*, pages 672–677 vol.1, June 1991.

[Chiaverini *et al.*, 1994] S. Chiaverini, B. Siciliano, and O. Egeland. Review of the damped least-squares inverse kinematics with experiments on an industrial robot manipulator. *IEEE Transactions on Control Systems Technology*, 2(2):123–134, Jun 1994.

[Cloutier *et al.*, 1994] Guy M. Cloutier, Alain Jutard, and Maurice Btemps. A robot-task conformance index for the design of robotized cells. *Robotics and Autonomous Systems*, 13(4):233 – 243, 1994.

[Dong *et al.*, 2017] X. Dong, D. Axinte, D. Palmer, S. Cobos, M. Raffles, A. Rabani, and J. Kell. Development of a slender continuum robotic system for on-wing inspection/repair of gas turbine engines. *Robotics and Computer-Integrated Manufacturing*, 44(Supplement C):218 – 229, 2017.

[Dubey and Luh, 1988] Rajiv Dubey and John Y. S. Luh. Redundant robot control using task based performance measures. *Journal of Robotic Systems*, 5(5):409–432, 1988.

[Hashimoto, 1985] Ryoichi Hashimoto. Harmonic mean type manipulatability index of robotic arms. *Transactions of the Society of Instrument and Control Engineers*, 21(12):1351–1353, 1985.

[Horigome *et al.*, 2014] A. Horigome, H. Yamada, G. Endo, S. Sen, S. Hirose, and E. F. Fukushima. Development of a coupled tendon-driven 3D multijoint manipulator. In *2014 IEEE International Conference on Robotics and Automation (ICRA)*, pages 5915–5920, May 2014.

[Kim and Khosla, 1991] Jin-Oh Kim and K. Khosla. Dexterity measures for design and control of manipulators. In *Intelligent Robots and Systems '91. 'Intelligence for Mechanical Systems, Proceedings IROS '91. IEEE/RSJ International Workshop on*, pages 758–763 vol.2, Nov 1991.

[Kucuk and Bingul, 2006] Serdar Kucuk and Zafer Bingul. Comparative study of performance indices for fundamental robot manipulators. *Robotics and Autonomous Systems*, 54(7):567 – 573, 2006.

[Marais and Göktoğan, 2017] Wilhelm Johan Marais and Ali Haydar Göktoğan. Design and control of CRAM: A highly articulated cable-driven remote access manipulator for confined space inspection. In *Australasian Conference on Robotics and Automation (ACRA-2017)*, page 9pg., Dec 2017.

[Mayorga *et al.*, 1992] R. V. Mayorga, A. K. C. Wong, and N. Milano. A fast procedure for manipulator inverse kinematics evaluation and pseudoinverse robustness. *IEEE Transactions on Systems, Man, and Cybernetics*, 22(4):790–798, Jul 1992.

[Patel and Sobh, 2015] Sarosh Patel and Tarek Sobh. Manipulator performance measures - a comprehensive literature survey. *Journal of Intelligent & Robotic Systems*, 77(3):547–570, Mar 2015.

[S. Hirose, 1991] S. Ma S. Hirose. Coupled tendon-driven multijoint manipulator. In *Proceedings of 1991 IEEE International Conference on Robotics and Automation*, volume 2, pages 1268 – 1275, April 1991.

[Yoshikawa, 1985] Tsuneo Yoshikawa. Manipulability of robotic mechanisms. *The International Journal of Robotics Research*, 4(2):3–9, 1985.